Article

Interfacial Properties and Emulsification of Biocompatible Liquid-Liquid Systems

Katarzyna Dziza [1] , **Eva Santini** [1] , **Libero Liggieri** [1,]*, **Ewelina Jarek** [2] , **Marcel Krzan** [2] , **Thilo Fischer** [3] **and Francesca Ravera** [1]

[1] Institute of Condensed Matter Chemistry and Technologies for Energy, Unit of Genoa, 16149 Genoa, Italy; katarzyna.dziza@ge.icmate.cnr.it (K.D.); eva.santini@ge.icmate.cnr.it (E.S.); francesca.ravera@ge.icmate.cnr.it (F.R.)

[2] Jerzy Haber Institute of Catalysis and Surface Chemistry, Polish Academy of Sciences, 30-239 Krakow, Poland; ncjarek@cyf-kr.edu.pl (E.J.); nckrzan@cyf-kr.edu.pl (M.K.)

[3] 4GENE GmbH, 85354 Freising, Germany; thilo.fischer@4gene.de

* Correspondence: libero.liggieri@ge.icmate.cnr.it

Abstract: A comparative study is reported on the interfacial properties of a set of surfactants and is discussed in terms of the effects on the features of the corresponding oil-water emulsions. The surfactants are saponin, Tween 80 and citronellol glucoside (CG), while the oil is Miglyol 812N—A Medium Chain Triglyceride (MCT) oil. Due to their high biocompatibility, all these compounds are variously utilized in food, cosmetic or pharmaceutical products. Among the surfactants, which are all soluble in water, CG presents also an important solubility in oil, as shown by the measured partition coefficient. For these systems, dynamic and equilibrium interfacial tensions and dilational viscoelasticity are measured as a function of the surfactant concentration and analyzed according to available adsorption models. In order to compare these results with the time evolution of the corresponding emulsions, the actual surfactant concentration in the matrix phase of the emulsion is accounted for. This may differ significantly from the nominal concentration of the solutions before dispersing them, because of the huge area of droplets available for surfactant adsorption in the emulsion. Using this approach allows the derivation of the correlations between the observed emulsion behavior and the actual surfactant coverage of the droplet interface.

Keywords: interfacial tensions; dilational rheology; biocompatible emulsions; partition coefficient; Tween 80; saponin; citronellol glucoside; MCT oil; Miglyol 812N

1. Introduction

Emulsions in cosmetic, pharmaceutical and food industry rely on biocompatible formulations. Among the various ingredients, surfactants are needed to provide long term stability and suitable features (drop size and distribution, tactile and sensorial attributes, etc.) to the emulsified products. Aiming at these applications and, more generally, to pursue the objectives related to green and sustainable development, surfactants derived from plant products are more and more utilized, in substitution of synthetic and even biocompatible molecules.

The present paper addresses the interfacial properties and emulsification of water-oil system for two surfactants derived from vegetable sources, namely saponin and citronellol glucoside (CG) as compared to the classical biocompatible synthetic surfactant Tween 80.

As the biocompatible oil phase the Medium Chain Triglyceride (MCT) oil is used. MCT is a coconut-oil derivate which, owing to its purity and high and well-defined content of saturated triglycerides, which are metabolized in an easy way by the body, is largely utilized in pharmaceutics

and is receiving increasing attention from nutritionists. Applications are therefore also devised by food and cosmetic industry. Emulsions of MCT find, in particular, interesting applications in the development of effective parenteral nutrition formulations, nutraceutics and for the encapsulation of active ingredients and drugs [1–4]. The formulation of fully biocompatible emulsions of MCT represents therefore a valuable target for many applications.

Saponin is a natural surfactant mainly extracted from plants [5,6] characterized, in general, by a hydrophobic aglycone structure with hydrophilic sugar residues. Many species of saponin exist, mostly classified on the basis either of the differences in the aglycone structure or the number of linked sugar chains [7]. The adsorption properties of saponin at water-air interface in relation to its ability to stabilize foams have been widely investigated [8–11]. In particular, it has been evidenced that the appreciable surface activity of saponin at water-air interface together with high value of the dilational viscoelasticity modulus, which has been found to be of the order of hundreds mN/m [8], make this compound a rather effective stabilizer of foams, already in pure water, without any further additives. Recently, saponin is intensively studied also as an emulsifying and emulsion stabilizing agent [12–15].

Citronellol glucoside (CG) is the β-D-glucoside of citronellol, an unsaturated monoterpene widespread in plant essential oils and a common flavor used in cosmetics and body care, as well as an aroma compound of food (Citrus sensation). Its glucoside CG is also occurring in crop plants like grape as a storage form of aroma. Recently, it became available by biotechnological production and can serve a dual role as a flavor precursor split by enzymes (e.g., in oral cavity) and as a non-ionic tenside or emulsifier in consumer products. CG is less complex in comparison to saponin with respect to chemical structure(s) and chemical identity. The aglycon of CG is a monoterpene (C10, branched alkene), while that of saponin is a triterpene (C30, substituted ring structures); the glycosidic parts are monosaccharides in the case of CG, while they are oligosaccharides in case of saponin, containing also an ionic carboxy-function. Furthermore, saponin is a mixture of triterpene glycosides.

Tween surfactants belong to a class of synthetic non-ionic surfactants which are considered non-toxic and to weakly interact with electrolytes and, for that, widely employed in those fields requiring bio-compatibly as emulsion stabilizers, both for domestic use and industrial application [16,17]. Moreover, they are often used as model surfactants in fundamental studies on emulsification and coalescence [18]. In particular, Tween 80 (polyoxyethylene sorbitan monooleate) is a synthetic non-ionic tenside or emulsifier and is composed of a central sorbitol (anhydride) structure derivatized from polyoxyethylene chains and the oleate ester group, the latter representing the lipophilic part of the molecule. It is in wide use in food, cosmetics and pharmacy technology.

Even though surfactants are key ingredients for emulsifiers, there is still a lack of deterministic approaches for the formulation of emulsions with desired characteristics, on the basis of the properties of concerned surfactant adsorption layers. This represents a challenging task, requiring systematic investigations contributing to clarify how the properties measured for single interfaces correlate for example with the stability and the drop size evolution of corresponding emulsions.

Based on these premises, a study on the interfacial properties of the above described surfactants at water-MCT oil interfaces, in relation to their ability to stabilize emulsions, is here presented. The interfacial characterization is carried out by interfacial tension and dilational viscoelasticity measurements, with the aim of assessing the adsorption properties of the different surfactants from the point of view of both thermodynamics, determining the equilibrium relation between the bulk concentration and the adsorption or adsorption isotherm and dynamics, evaluating the dilational rheology response of the adsorbed layers. These properties are then correlated with the behavior of the respective emulsions, monitored during their evolution and analyzed in terms of their structure by optical microscopy observation.

The mitigation of potential adverse impacts of emulsifiers on environment and health is pursued not only by the use of biocompatible surfactants but also by the reduction of their amount in the formulations. At low surfactants concentrations however, the process of emulsification in micro- and sub-micro-sized droplets results in a significant depletion of the surfactant concentration in the liquid

phases, caused by the adsorption at the huge amount of liquid-liquid interfacial area produced. The proper correlation between interfacial properties and emulsion features needs then to account for these depletion effects. These aspects, however, have not received so far sufficient attention in the available studies, while they are explicitly accounted for and discussed in the present one.

2. Background on Emulsions and Droplet Interfacial Properties

The relationship between the interfacial properties of adsorbed layers at liquid-liquid interfaces and the process of emulsification and emulsion stability is well-recognized [19,20].

Emulsification is the production of small droplets by fragmentation of the oil phase with a consequent large increase of the surface area. For energetic reasons, it is favored by low surface tensions and fast adsorption processes. In fact, for a given energy provided to the system, smaller droplets are generated with surfactants that are more efficient to adsorb and reduce the interfacial tension. The aging of emulsions is governed by various processes influenced by the bulk and adsorption properties of surfactants, both at equilibrium and in dynamic conditions. These are creaming or sedimentation, which is the gravity-driven phase separation due to the density difference between the two liquids, Ostwald ripening and droplet coalescence [21]. Ostwald ripening consists in a partial dissolution of the dispersed liquid phase induced by the capillary pressure, which results in a net mass transfer from small to big droplets. This process mainly involves small droplets, because of their higher capillary pressure, and, for oils with low solubility in water, as it is case of long-chain alkanes [22,23], presents very long characteristic times. The emulsions reported here are obtained by a low-energy method and are therefore characterized by relatively big droplet sizes, for which Ostwald ripening has a negligible relevance for the emulsion ageing as compared to creaming and coalescence. Coalescence consists on the merging of two droplets into a single larger one, due to the complex hydrodynamic process of thinning and rupture of the liquid film between them. As a consequence of coalescence the droplet size distribution tends to be enlarged and moves towards larger sizes, eventually favoring creaming and destabilization of the emulsion. Among the most important effects relevant for the hindering of droplet coalescence, it is worth to mention the repulsive interaction between adsorbed layers, the interfacial coverage, the steric effects and the high dilational viscoelasticity of the interfacial layers [24,25]. The repulsive interactions are particularly relevant when ionic surfactants are concerned. In that case, it has been shown that a small amount of adsorbed molecules at the drop surface is sufficient to avoid coalescence [25] and improve remarkably the stability of emulsions. The interfacial coverage is the relative area of the interface occupied by the surfactant. High values of this parameter represent another stabilizing factor against coalescence due to the short range interactions of the surfactant molecules adsorbed at the two sides of the film between droplets. Since the total area of the droplet interfaces decreases with droplet coalescence, the surface coverage increases and, when high values of it are achieved through this process, the coalescence eventually stops. Thus surface coverage is implied in determining the droplet size of stable emulsions. Steric effects are especially concerned with composite surface layers, such as surfactant-nanoparticle mixtures or surfactant aggregates but also with large surfactant molecules at high adsorption coverage.

The dilational viscoelasticity, E, is the dynamic response of the interfacial tension, γ, to extensional perturbations of the surface area, A. For small amplitude harmonic perturbations, E is a frequency dependent complex quantity, defined as:

$$E = \frac{\Delta\gamma}{\Delta A/A_0}e^{i\varphi} \tag{1}$$

where $\Delta\gamma$ and ΔA are the amplitudes of the oscillating surface tension and surface area, respectively, A_0 is the reference area and φ is the phase shift between the oscillating surface tension and surface area. According to its definition, high values of the dilational viscoelasticity tend to make the liquid films between drops in emulsions more stable and, in particular, to hinder their local thinning for Marangoni effects.

From these considerations it is clear that a deep characterization of the surfactants used for stabilizing emulsions, at liquid-liquid interfaces, is of fundamental importance to understand the stabilizing mechanisms and the role of the different features of the used surfactants.

3. Materials and Methods

3.1. Materials

For all the experiments, ultrapure water—produced by a MilliRO plus MilliQ (Millipore, Burlington, MA, USA) system and characterized by resistivity larger than 18 MΩ·m—was used. Surface tension measurement provides a value of 72.5 ± 0.2 mN/m, stable for at least two hours at 20 °C meaning negligible amount of surface active impurities.

The Medium Chain Triglyceride (MCT) oil was Miglyol 812N, obtained from IOI OLEO (Hamburg, Germany) and utilized without further purification. Miglyol 812N contains about 95% of triglycerides of the fractionated C8 (50%–65%) and C10 (30%–45%) vegetable fatty acids. Lighter or heavier triglycerides compose the 5% left. The absence of surface active impurities in the used MCT oil was checked by interfacial tension measurements against water, which did not reveal any appreciable kinetics over some hours. At 20 °C the interfacial tension of 25.4 ± 0.2 mN/m was found, which is in agreement with the values available in the literature [17,26–28].

Saponin was reagent grade purchased from VWR (catalogue n. VWRV0163, Radnor, PA, USA) and utilized as supplied. This product has been used also in Reference [11], where its composition has been analyzed and discussed in detail. It is an extract from *Quillaia saponaria* containing a mixture of components with a rather broad distribution of molecular weights (from 1070 to 1700 g/mol). However, in order to analyze the adsorption properties of saponin, in comparison with the other surfactants investigated, we assume, like in many studies of saponin or mixtures of saponins [29–31], the value of 1650 g/mol as the average molecular weight. Moreover, from the results reported in Reference [11] for neutral pH, like in this work, saponin is expected to be predominantly dissociated and to behave as an ionic surfactant.

Tween 80 was purchased from Sigma Aldrich (St. Louis, MO, USA) and used as received. It is a non-ionic surfactant whose molecular weight and cmc are 1310 g/mol and 0.012 mM at 20–25 °C, respectively (as provided by the supplier).

Citronellol-β-ᴅ-glucoside, CG, was kindly supplied by the producer (4GENE GmbH, Freising, Germany), which also provided a value of the molecular weight equal to 318.39 g/mol and an estimation of the HLB and cmc, that are 11.3 and 0.01 M, respectively.

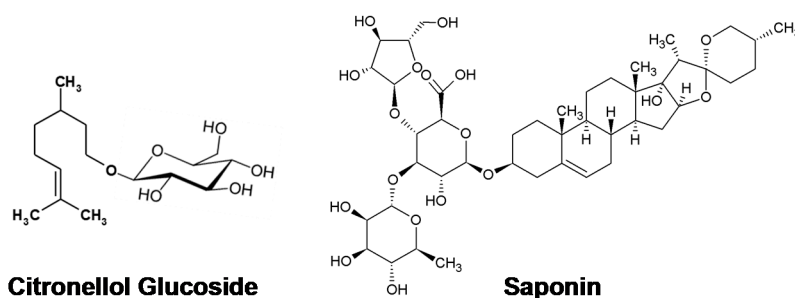The chemical formulas of saponin and CG are given in Figure 1.

Figure 1. Natural surfactants investigated in the study.

3.2. Methods

For the reported tensiometric experiments, the interfacial tensions were measured with a Pendant Drop Tensiometer (PAT1, Sinterface, Berlin, Germany). As described in large detail in Reference [32], the technique is based on the analysis of the shape of a pendant drop attached to a capillary. The shape of a drop results, in fact, from the competition between interfacial tension and gravity and

can be formally described by the Bashfort-Adams equation (B-A). In the utilized apparatus, the drop images are automatically acquired by a 1024×1024 pixels camera, equipped with a macro objective and interfaced to a PC. Then, the software of the apparatus fits the B-A equation to the coordinates of the drop profiles extracted from the acquired images, yielding the interfacial tension as one of the best fit parameters. Specifically, the PAT1 apparatus allows for an accurate control of the droplet area by a syringe pump, driven by a feedback loop software based on the drop imaging. Due to this feature, the tensiometer has been utilized to investigate the adsorption processes of the various surfactants by two types of measurements. The dynamic interfacial tension versus time on a freshly formed drop is measured during the ageing of the interface while keeping the drop area constant. The equilibrium interfacial tensions are obtained from these data at long time. The measurement of the dilational viscoelasticity is instead performed according to the oscillating drop method [33]. For this latter, harmonic perturbations of the droplet area are applied once the adsorption equilibrium is achieved. The amplitude of the area oscillation is typically 2% and the frequency range from 0.005 to 0.2 Hz, to warrant the quasi-equilibrium mechanical condition and the linearity of the rheological response, respectively. For each frequency, amplitude and phase of the measured interfacial tension and area signals during the oscillations are calculated by standard Fourier analysis methods and utilized to obtain the dilational viscoelasticity according to Equation (1). Full details on this measurement method and on the appropriate conditions for its applicability are reported elsewhere [34].

Notice that, in order to minimize the possible depletion of the surfactant solution caused by the adsorption itself or by the surfactant transfer into the oil phase (if any partitioning may exist), in all the reported cases the measurement refers to emerging drops of oil (from 30 to 50 mm^3, depending on the surfactant and on its concentration) inside the surfactant aqueous solution.

Emulsions were produced according to a Double Syringe (DS) method. This method, developed and mainly used for foams [11,35], is here adapted for investigating emulsions. In this technique, emulsions are obtained by repetitive exchanging of the liquids between two syringes connected by a short narrow pipe. In this way, the emulsion is formed by the turbulent flow caused by the shearing inside the pipe.

For the tests reported here, two 5 mL standard syringes connected through a rigid 15 mm long pipe and with an inner diameter of 1 mm were used. Each syringe initially contained a volume of 2.5 mL of one liquid phase, aqueous surfactant solution and oil, so that the water-oil volume ratio was $V_{oil}{:}V_{water} = 1{:}1$ for all the emulsions investigated.

To produce the emulsions, twenty sequential cycles were applied consisting of a pushing of the liquid/liquid mixture through the connector from one syringe to the other one. Like in the previous work on foams [11], the number of cycles was optimized to maximize the emulsification obtaining, at the same time, emulsion stability appropriate to perform comparative investigations varying the type of surfactant and the concentration. After formation, the syringes containing the emulsions were stored in a vertical position and monitored for at least two days, measuring the heights of the emulsion and of the separating phases by using a ruler, with a resolution of 0.5 mm.

The size of the droplets in the emulsions, produced by the DS method, were evaluated using the reflected light DVM6-M microscope (Leica, Hamburg, Germany) fitted with the PlanAPO FOV 3.60 objective, warranting a resolution better than 1 micron. For this purpose, small amounts of emulsion (~0.1 mL) taken directly from the syringe immediately after the emulsification and diluted 10 times with the corresponding surfactant solution, were placed between two glass slides separated by a spacer of 0.2 mm thickness to be observed. That allows to distance the emulsion droplets, easing the analysis of the droplet size distribution on the captured microscope images. The droplet radii are obtained by the analysis of these images by purposely available routines of the proprietary microscope software (Leica LAS X, v.3.7.1).

4. Results

4.1. Interfacial Properties

The interfacial tension of surfactant solutions against the MCT oil has been measured at various concentrations in water according to the method described in the previous section. In particular, the measurement of interfacial tension begins just after the formation of a "fresh" droplet interface—that is, an interface with an initially negligible amount of an adsorbed surfactant—and continues during the advancement of the surfactant adsorption process until the achievement of the equilibrium. This kind of measurements, apart from providing information on the adsorption kinetics such as, for example, the adsorption characteristic time, allows determining the equilibrium interfacial tension versus the bulk concentration, which characterizes the thermodynamic adsorption properties of an examined surfactant system. For all the cases investigated, after about two hours from the creation of the interface, the adsorption equilibrium may be assumed to be achieved, as the interfacial tension presents a variation lower than 1 mN/m in one hour. Figure 2 shows the interfacial tension versus time obtained for saponin at various bulk concentrations in water. The corresponding equilibrium interfacial tensions versus concentration are reported in Figure 3.
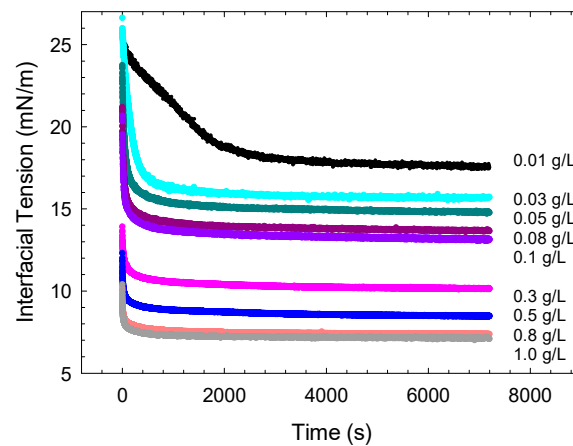
Figure 2. Interfacial tension versus time during the adsorption of saponin at water/Medium Chain Triglyceride (MCT) interface, for different concentrations of saponin in water: from 0.01 to 1 g/L.
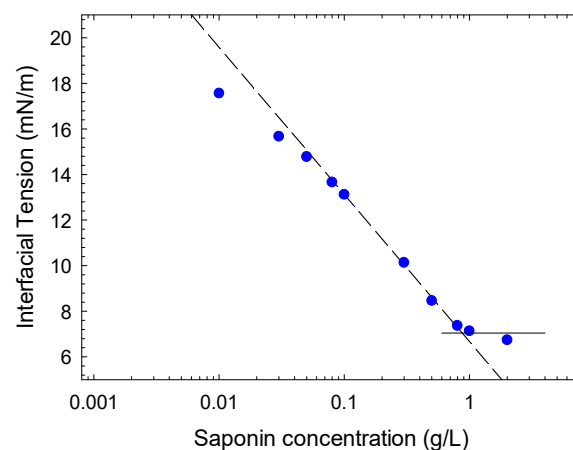
Figure 3. Equilibrium interfacial tension versus saponin concentration (symbols) and linear fitting of the experimental data close to the cmc providing through Equation (1) the maximum adsorption Γ_{max} = 2.6 μM/m^2.

From Figure 3 the achievement of the critical micellar concentration around 0.8 g/L (4.8×10^{-4} M, assuming 1650 g/mol as molecular weight) is evident. This value is in agreement with that found for the same type of saponin in Reference [11], from surface tension measurements at water-air interface.

The slope of the best fit line at concentrations (*C*) approaching the cmc, provides the maximum value of the adsorption at the water-MCT interface, through the Gibbs adsorption isotherm:

$$\Gamma = -\frac{1}{RT}\frac{\partial \gamma}{\partial \ln C} \tag{2}$$

where *T* is the temperature and R the gas constant, which provides a value for the maximum adsorption of 2.6 ± 0.1 μmol/m^2. This adsorption value is much lower than that found in Reference [11], for the water-air interfaces, that is 5.1 μmol/m^2. This can be due to the lower affinity of saponin molecules with the water-oil interface or to a much higher occupational area of the adsorbed saponin molecules caused by a different placement of the saponin molecule at the interface between oil and water.

Figure 4 reports the equilibrium interfacial tension versus the molar concentration of surfactants in water for the three systems investigated in this work. The continuous curves reported in the figure for saponin and Tween 80 are the best fit theoretical *γ-c* isotherms from the reorientation adsorption model [36,37]. According to this model, the surfactant molecules may adsorb assuming different orientation with respect to the interface, corresponding to different occupational area. The average area per mole, ω, may be expressed through two parameters, ω_1 and ω_2, corresponding to the orientations which make maximum and minimum the molecular area, respectively. That is:

$$\omega = \frac{\omega_1\left(\frac{\omega_1}{\omega_2}\right)^{\alpha} e^{-\frac{\Pi(\omega_1-\omega_2)}{RT}} + \omega_2}{1 + \left(\frac{\omega_1}{\omega_2}\right)^{\alpha} e^{-\frac{\Pi(\omega_1-\omega_2)}{RT}}} \tag{3}$$

where Π is the surface pressure, $\Pi = \gamma_0 - \gamma$, which is strictly related to the total adsorption Γ, through:

$$\Pi = -\frac{RT}{\omega}\ln(1 - \Gamma\omega) \tag{4}$$
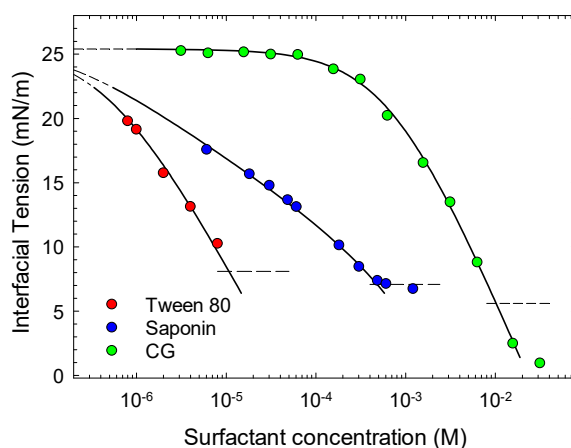
Figure 4. Equilibrium interfacial tension versus molar surfactant concentration in water (for saponin calculated assuming 1650 g/mol as molar weight) and respective best fit isotherm curves (Equations (3)–(5)).

This model provides, moreover, the following equilibrium relation between the interfacial tension and the bulk surfactant concentration, c:

$$bc = \frac{1 - e^{-\frac{\Pi \omega}{RT}}}{\left(\frac{\omega_1}{\omega_2}\right)^{\alpha} e^{-\frac{\Pi \omega_1}{RT}} + e^{-\frac{\Pi \omega_2}{RT}}}$$

(5)

where b and α are two parameters related to the surface activity of the two orientation states which, together with ω_1 and ω_2, completely describe the equilibrium adsorption properties of the system.

Notice that this model is essentially an extension of the Langmuir model where only one molar surface area is considered in the whole bulk concentration range investigated. The value of the molar area, ω, in this case also defines the saturation adsorption $\Gamma_{sat} = 1/\omega$.

As shown in Figure 4, Equation (5) fits well the equilibrium interfacial tension data obtained for saponin and Tween 80, while the CG behavior is well-described by a Langmuir isotherm. In fact, for all cases the weighted average standard deviation between the calculated and measured values is lower than 0.05, which is considered more than satisfactory. The best fit values are reported in Table 1. The surface activities of the different compounds are expressed through the values of b which change by two orders of magnitude passing from CG to Tween 80. Similar values are found for ω_2 which is related to the saturation adsorption, that is $\Gamma_{sat} = 1/\omega_2$. The tendency of the adsorbed molecules to re-orient found for saponin and Tween 80 is coherent with the more complex structure of these molecules with respect to CG, while the values of ω_1 reflect their difference in molecular weight and size.

Table 1. Adsorption isotherm parameters corresponding to the best fit curves reported in Figure 4 and critical micellar concentration, cmc.

Surfactant	ω_1 (m²/mol)	ω_2 (m²/mol)	b (m³/mol)	α	cmc (M)
Tween 80	5.60×10^5	3.80×10^5	8.69×10^2	0.6	1.2×10^{-5} [a]
Saponin	1.20×10^6	3.60×10^5	15.2	4.4	4.8×10^{-4} [b]
CG	–	3.4×10^5	1.43	–	1.0×10^{-2} [a]

[a] from producer; [b] from interfacial tension measurements.

Notice that, in the case of saponin, the peculiarity of reorienting at the interface explains the different values of maximum adsorption that such surfactant may assume when different interfaces are involved like in the above- reported case of water-air interface.

4.2. Partitioning

When surfactants are investigated at a liquid-liquid interface an important aspect to be taken into account is the possible partitioning between the two liquid phases. In our cases, the transfer of the surfactant across the water-oil interfaces and the possible impoverishment of one phase with respect to the other one, may play an important role in the dynamics of the adsorption as well as in the features of the obtained emulsions. This phenomenon has been widely investigated [38] and methods to evaluate the partition coefficient, that is the ratio between the equilibrium surfactant concentrations in oil and water phases, have been developed [39,40].

The partitioning can be especially relevant for Tween 80 and CG that are non-ionic surfactants, while, we can expect the transfer into the oil phase to be negligible for saponin. In fact, according to the results reported in Reference [11], for neutral pH, like in the present case, saponin is predominantly dissociated and behaves therefore as an ionic surfactant.

An effective way to assess the possible surfactant transfer across the interface is to compare the behavior of the dynamic interfacial tension obtained with a drop of oil immersed in the aqueous surfactant solution with that obtained with the opposite configuration, that is a pendant drop of solution in an initially surfactant-free oil phase. In the second case, due to the much higher volume of the oil phase, the transfer provides the typical minimum trend of the interfacial tension [38].

For saponin and Tween 80 this test indicated negligible solubility of surfactant in MCT, resulting in an almost coincident dynamic interfacial tension variations found in the two different configurations. On the contrary, the dynamic interfacial tension of a drop of GC aqueous solution in MCT shows an evident minimum, as illustrated in Figure 5, indicating the transfer of CG into the oil phase.
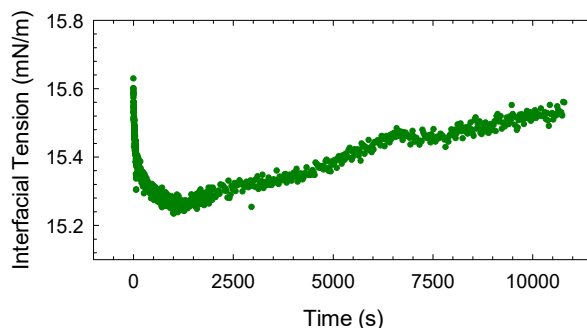
Figure 5. Dynamic interfacial tension versus time obtained with a pendant drop of aqueous solution of citronellol glucoside (CG at $c = 7.6 \times 10^{-4}$ M inside an initially pure MCT phase.

To evaluate the partition coefficient $K_p = c_w/c_{MCT}$, we have adopted the method described in Reference [40]. Accordingly, CG solution in MCT are prepared and the equilibrium interfacial tensions measured using a pendant drop of initially pure water immersed in such solutions. The comparison of these data with the adsorption isotherm obtained in the opposite configuration, that is, equilibrium interfacial tension versus concentration in water, provides for each value of the interfacial tension (see Figure 6) the two concentrations in partition equilibrium. Using the data in Figure 6, the partition coefficient of CG was estimated as $K_p = 0.42 \pm 0.05$, where the value and the uncertainty are obtained by the average of the K_p's determined by the couples of concentrations at the various interfacial tensions.
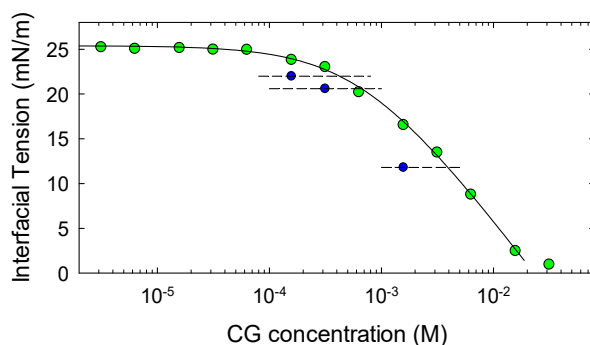
Figure 6. Equilibrium interfacial tension versus molar CG concentration in MCT (blue symbols) and in water (green symbols).

4.3. Dilational Rheology

The dilational viscoelasticity versus frequency of the above-investigated systems has been measured according to the oscillating drop method, as described in Section 3.2, in a range of concentration in water below the cmc where the concentration dependence of the equilibrium interfacial tension is appreciable. Figure 7 reports the results obtained for saponin and Tween 80. For CG, lower values of the dilational viscoelasticity modulus were found, around 4 mN/m and below, without a significant trend with frequency and, for this reason, they are not reported in Figure 7.
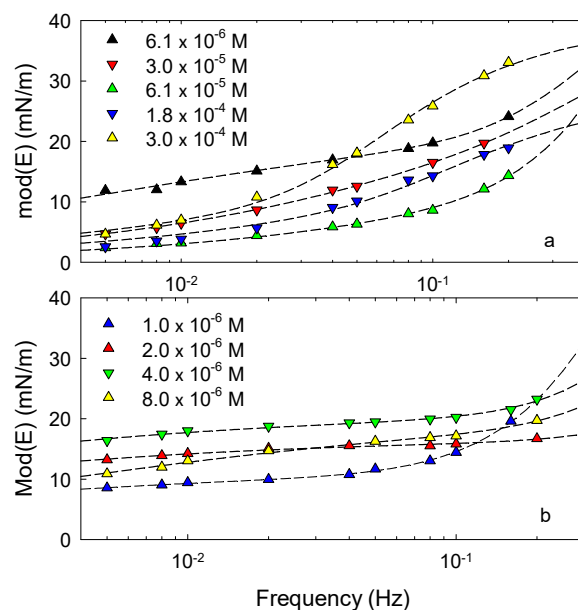
Figure 7. Modulus of the dilational viscoelasticity measured by the Oscillating Drop method for saponin (**a**) and for Tween 80 (**b**). Dashed curves obtained fitting a theoretical expression of mod(E) like in Reference [25] from the model presented in Reference [41].

For saponin and Tween 80 the trend of the dilational viscoelasticity versus frequency is that typical of soluble surfactants at liquid interfaces. The data are, in fact, well fitted by theoretical curves obtained assuming a general model taking into account the bulk diffusion and a re-arrangement process in the adsorbed layer [41]. For these surfactants, on the basis of the results reported in the previous section, this interfacial process is expected to be related to the variation of the average molecular orientation in the adsorbed layer.

In many studies on interfacial rheology of surfactants at liquid interfaces [25,42,43], using this model to interpret the experimental data has been effective to understand the mechanisms governing the adsorption process and to evaluate the associated kinetic parameters. For the systems here investigated, however, the frequency range used is probably not wide enough to provide an accurate description of their dynamic behavior and consequently quantitative information on the processes occurring in the adsorbed layers. Despite this limitation, these results, even if concerned with low frequency perturbations, give important information on the rheological properties of the adsorbed layers and evidence the differences between the investigated surfactants. One difference concerns the values of the dilational viscoelasticity for saponin and Tween 80 which are similar to those of common low-weight surfactants at liquid-liquid interfaces [25,44], while, in comparison, the rheological response of CG is negligible. Moreover, for saponin the increasing rate of the viscoelastic modulus with frequency is higher than that observed for Tween 80. This implies that in the case of saponin much higher values can probably be reached at high frequency.

It is interesting to notice that, as found in previous studies [11,29,30], for saponin at water-air interface the viscoelasticity modulus reaches very high values, compared with common surfactants, already for frequencies below 0.2 Hz. This peculiarity, not observed here for water-MCT interfaces, was associated with the good ability of this natural surfactant to stabilize foams. This means that the better ability of saponin as emulsion stabilizer, compared to the other surfactants, reported in the next section, should be attributed to the not directly observed high frequency elasticity or to other molecular features of saponin such as the higher molar area and the ionic character.

4.4. Emulsions

In order to compare the effectiveness of the different surfactants as emulsion stabilizers and to evidence the effects of their concentrations, all emulsions were produced following exactly the same procedure, that is the double syringe method as described in Section 3.2. These water-in-oil emulsions were then monitored for 2 days by measuring the relative emulsion volume, V_{em}/V_{total}. The results obtained for all surfactants and concentrations are summarized in Figure 8, where the concentrations correspond to those of the aqueous solutions before emulsification.
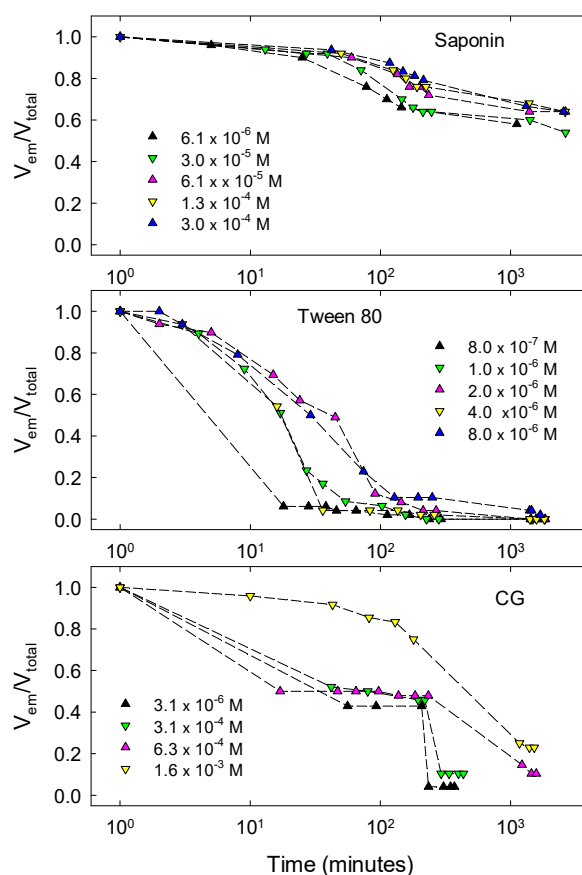

Figure 8. Evolution of the relative oil-in-water emulsion volume for different concentrations of the aqueous surfactant solution before emulsification. Results obtained by the Double Syringe technique using two 5 mL syringes, 20 manual pushing cycles and volume ratio V_{oil}:V_{water} = 1:1.

In all the cases reported a total emulsification of the samples was observed, that is, V_{em}/V_{total} = 1 at the initial time of the emulsion monitoring. Afterwards, emulsions evolve with different trends depending on the surfactants used. As shown in Figure 8, saponin-stabilized emulsions present a slow reduction of the volume during the first two days from the formation, with a slight dependence on the concentration. For the lowest concentration investigated, that is, 6.1×10^{-6} M, a small volume of MCT phase starts to separate after about one day from the formation, reducing the emulsion volume. For the higher concentrations, instead, the MCT phase remains totally emulsified for several days (more than 15), with the relative emulsion volume which after the reduction of the first two days maintains constant at $V_{em}/V_{total} \approx 0.6$. The fact that no separated oil phase appears means that coalescence of MCT droplets is hindered by saponin adsorbed layers and the initial reduction of the emulsion volume is mainly due to an increased droplet compactness related to the aqueous phase drainage.

Tween 80-stabilized emulsions are appreciably less stable than those with saponin. This is not only evidenced by the faster reduction of the emulsion volume (see Figure 8) but also by the fact that, for all the concentrations studied, a separated oil phase appears and grows on the top of the emulsions

already after 10 min from the formation. This means that Tween 80 under these conditions is not an efficient stabilizer against coalescence. The emulsions stabilized by CG present a more complex behavior where the time evolution of the emulsion volume significantly depends on the concentration. For this surfactant, like for Tween 80, the reduction of the emulsion volume is associated with the appearance of a separated MCT phase meaning that, also in this case, the droplet coalescence has an important role in the destabilization. Moreover, as evident from Figure 8, only for the emulsions obtained with the highest concentration, that is, 1.6×10^{-3} M, the destabilization is rather slow, during the monitoring time. For the other concentrations investigated, the emulsion volume is reduced by half in about ten minutes maintaining rather constant for several hours before a drastic fall after about one day. In correspondence with this abrupt volume reduction the appearance of a new turbid thin phase is visually observed, just above the emulsion, below the separated MCT phase, with a small volume not easy to evaluate. This particular behavior of the CG-stabilized emulsions as well as the appearance of this new phase during their evolution, is possibly related to the solubility of this surfactant in both water and oil phases. On the basis of the value of the partition coefficient indicated in the previous section, one can suppose that the new phase observed could be a water-in-oil emulsion coexisting with the principal oil-in-water ones. The analysis of these latter ones by optical microscopy gives information that support this hypothesis. In fact, from the image reported in Figure 9 of a typical emulsion obtained with CG, it is evident that a multiple emulsion is produced, where the droplets are, in turn, a disperse water-in-oil phase.
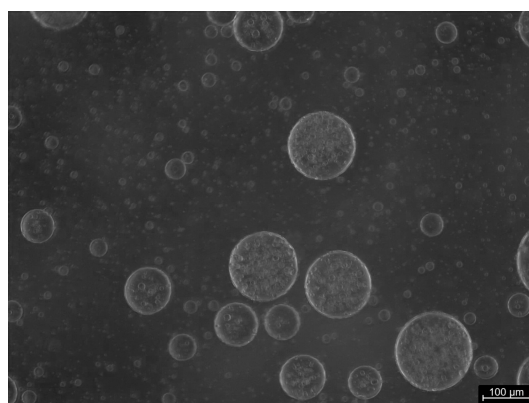

Figure 9. Typical microscope image of an emulsion stabilized by CG at 6.2×10^{-4} M, where the composite feature of the disperse phase is evident.

The emulsions were also analyzed by optical microscopy at the beginning of their evolution, when they are completely emulsified. Figure 10 shows some examples of size distribution obtained by this analysis. In general, the droplets resulted to have a radius distributed in a range from 2 to 15 micron with the average value between 4 and 9 microns, depending on the surfactant type and concentration. Considering the simple emulsification method, the width of these distributions is therefore rather narrow. Moreover, the droplet sizes observed confirm that Ostwald ripening does not play a relevant role over the timescale investigated, so that the change in V_{em} can be attributed to the combined effect of creaming, drainage and droplet coalescence.

In order to summarize the properties of the emulsions obtained with the different surfactants, we report in Figure 11 the relative emulsion volume, V_{em}/V_{total}, reached after one hour from the formation as a function of the surfactant concentration in water before emulsification (panel a) and the corresponding average droplet radius obtained from the size distributions by microscopy analysis (panel b). Apart from the highest concentration of CG, these data evidence a slight decrease of the average droplet size with the concentration and a general tendency to improve the stability with the decrease of the droplet size.
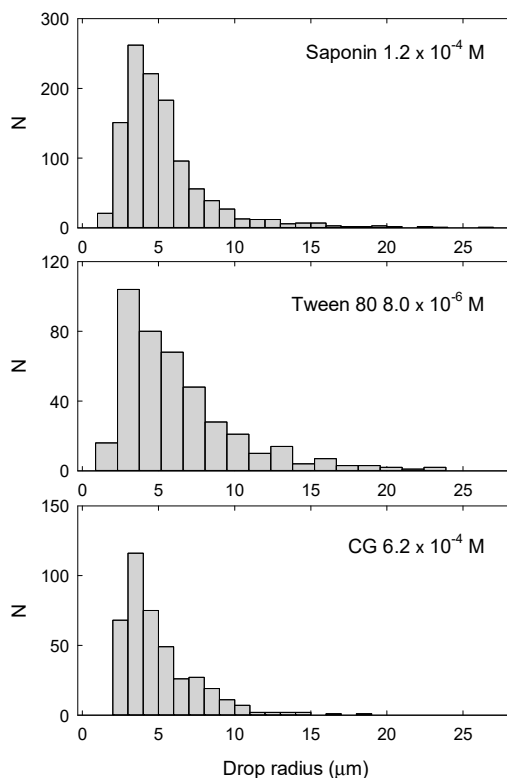
Figure 10. Examples of drop radius distributions from the microscope images acquired just after emulsification for the different surfactants.
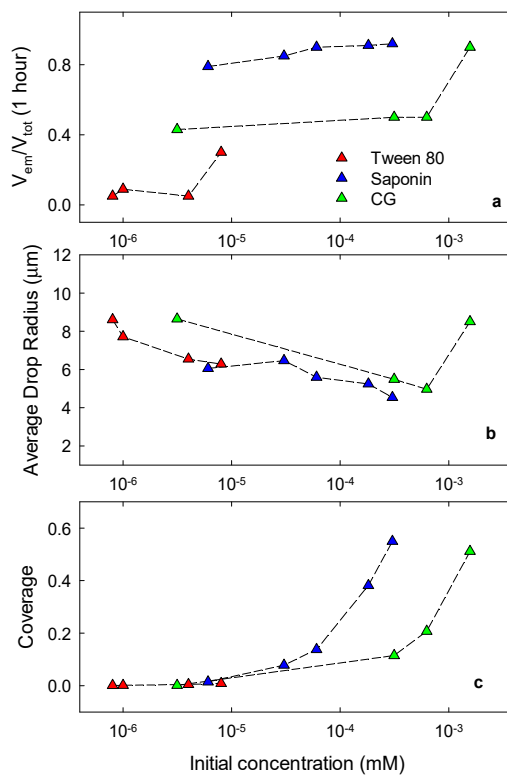
Figure 11. Relative emulsion volume at one hour from the emulsification (**a**), average emulsion drop radius obtained by microscopy images just after the emulsification (**b**) and surface coverage of oil drops in emulsions by the adsorbed surfactant (**c**), against the surfactant concentration in water before emulsification.

5. Discussion

The surfactants here investigated present different features as emulsion stabilizers that can be related to their adsorption properties at the surface of the dispersed MCT droplet after emulsification. During the emulsification process, however, the water-oil interface undergoes a huge area increase resulting in a significant depletion of the aqueous matrix phase induced by the adsorption. This effect is recognized to be very important to investigate the correlation between the interfacial properties and the stability of the corresponding disperse system. In fact, only accounting for this effect it is possible to evaluate the real surfactant adsorption onto the oil droplet surface in emulsions which is related, through the adsorption isotherm, to the real bulk concentration in water.

The calculation of the above depletion can be done by coupling the surfactant mass balance with the equilibrium adsorption isotherm. In our specific case, considering also the surfactant partitioning ($k = c_{oil}/c_{water}$) between the two liquid phases, the mass balance reads:

$$A\Gamma + cV_w\left(1 + k\frac{V_{oil}}{V_w}\right) = c_0 V_w \qquad (6)$$

where c is the concentration achieved after emulsification of oil and water volumes, V_{oil} and V_w, c_0 the initial concentration of the aqueous phase and A the total interfacial area that, assuming the complete emulsification of the oil volume in drops with average radius R, can be estimated as $A = 3V_{oil}/R$. Thus, coupling this balance of mass with the Γ-c equilibrium relation, provided by the adsorption isotherm, it is possible to obtain the value of Γ and of the coverage $\omega\Gamma$. The steps of this calculation are reported in more detail in Appendix A. Figure 11c shows the coverage for the three surfactants as a function of the initial concentration in water, calculated using the isotherm parameters found by the analysis of the equilibrium interfacial properties (Table 1) and the average drop radius as obtained by the droplet size distributions (Figure 11b). These data are also reported in Table A1 of the Appendix A.

From these results it is possible to evidence the main differences in the features of the surfactant investigated. It is important to underline again that, in order to obtain reliable comparative results, emulsions have been produced following exactly the same procedure. Emulsions stabilized by saponin are definitely more stable with respect to others and this is expected to be mainly due to the ionic character of this surfactant. In fact, it is well known that ionic surfactants are effective to hinder coalescence in emulsions due to the electrostatic repulsion between the surfactant layers at the two sides of the liquid film between droplets. Nevertheless, the results reported here suggest further reasons that can increase the stabilizing effects, related to the possibility for the large size surfactant molecules to reorient, which provides a large coverage already at low concentration. The evident low ability of Tween 80 as an emulsion stabilizer is surely due to the very low adsorption that can be achieved with this system at the surface of the MCT droplets. In fact, in this case the coverage is very low and the surfactant is non-ionic, hence it is not sufficient to hinder coalescence. Coalescence for this system can possibly occur also during the emulsification process and this could be the reason for the larger size of the drop at the beginning of the emulsion evolution with respect to the other surfactants. The behavior of CG-stabilized emulsions is surely the most complex. The principal reasons for the general unstable behavior of these emulsions are probably the low coverage that, together with the non-ionic character of the surfactant and negligible dilational elasticity of the adsorbed layer, makes this system not appropriate to hinder the droplet coalescence. Moreover, for this system an important role is played by the transfer of surfactants into the MCT phase, that can induce the formation of double emulsions or inverse water-in-oil emulsions which may be a further reason for the observed emulsion instability. However, increasing the CG concentration, such ability to form double emulsions may lead to the formation of more complex disperse systems characterized by a better stability. For example, the more stable emulsion obtained with the highest CG concentration (1.6×10^{-3} M) may be a dispersion of large aggregates of water droplets in MCT. Deeper investigations on this surfactant are surely required to better understand its behavior and its potentiality as a natural emulsion stabilizer.

Using the average drop radius in the estimation of the available interfacial area in the emulsion, for obtaining the data in Figure 11, is clearly a first order approximation. A more accurate estimation of *A* could be obtained accounting for the droplet size distributions, where available, according to the calculations given in the Appendix A. However, for rather narrow distributions, as in our case, the general conclusions of the above discussion would not change.

As a last point, it can be said that for the systems investigated in this work, the rheological properties of the adsorbed layers at the water-MCT interface seems to have only a marginal relationship with the stabilization of the corresponding emulsions. The negligible values of the dilational viscoelasticity for the CG system is associated with the unstable character of the corresponding emulsions. However, both Tween 80 and saponin present higher values but similar between them, even if their ability as emulsion stabilizers is very different. For these two surfactants a major role is played by the differences in the adsorption properties, ionic character and molar areas. In addition, the slight difference in the viscoelasticity trends, observed at low frequency, let us expect important differences in the rheological response in a higher frequency range.

6. Conclusions

We have investigated the properties of adsorption layers of different water-soluble biocompatible surfactants, namely Tween 80, saponin and citronellol glucoside at the interface between water and a Medium Chain Triglyceride oil, correlating them to the aging of corresponding emulsions.

The measured equilibrium interfacial tensions versus concentration for Tween 80 and saponin are well described within the framework of the reorientation model [37]. For CG the results are sufficiently well-described by the Langmuir model, for which the molar area of the adsorbed molecules is only one. This latter surfactant revealed also an appreciable solubility in MCT oil. The value of the partition coefficient has been then estimated and used in the interpretation of the behavior of the corresponding emulsions.

The results of the comparative emulsion study, performed for surfactant concentrations below the cmc and an observation time of two days, evidence different characteristics of the surfactants as emulsion stabilizers. According to these results, Tween 80 does not present, under the studied conditions, a good stability against droplet coalescence, so that the liquid phases are fully separated within about two hours. A good stability against coalescence is instead obtained with saponin. In fact, the corresponding emulsions, after an initial creaming, remain stable for at least 10 days, that is a time much longer than the observation time. CG emulsions present a relatively better stability only at the highest concentrations. The microscopy studies revealed, however, a much more complicated behavior of the emulsions with this surfactant since the formation of different phases and multiple emulsions was observed.

For the interpretation of these results, particular attention has been paid on the effect of the depletion of the surfactant concentration in the matrix phase of the emulsion caused by the increased available area for adsorption, induced by emulsification. Using the data of droplet sizes in emulsions, obtained by microscopy analysis and the eventual partitioning in the oil phase, such area has been evaluated and resulted to be more than significant. In fact, the observed behavior for the emulsions has been discussed and rationalized on the basis of the surfactant coverages at the droplet interface, corresponding to the real values of the concentrations resulting after emulsification. As expected, the emulsions showing a high stability against coalescence are those characterized by the larger coverages.

Concluding, the results of this work show that investigating both the adsorption properties of surfactants at liquid-liquid interfaces, by complementary techniques and the behavior of the corresponding emulsions, may be effective to determine in a comparative way the efficiency of new natural compounds. This may contribute to the development of innovative formulations of bio-compatible emulsions.

Author Contributions: Conceptualization, E.S., L.L., E.J., M.K. and F.R.; methodology, E.S., L.L., E.J., M.K. and F.R.; investigation, K.D., E.S., E.J. and M.K.; data curation, E.S. and K.D.; formal analysis F.R, M.K., T.F. and L.L.;

Appendix A. Calculations of the Surfactant Concentration Depletion Due to Adsorption on Emulsion Drops

After the formation of a new interface with area A, in a surfactant solution with the initial concentration c_0, an adsorption process starts and the system achieves a new equilibrium state, characterized by an adsorption Γ and a bulk concentration c, satisfying the set of equations provided by the mass balance and by the equilibrium adsorption isotherm:

$$\begin{cases} A\Gamma + cV = c_0 V \\ c = c(\Gamma) \end{cases} \tag{A1}$$

where V is the volume of the surfactant solution. Within the Langmuir model, the adsorption isotherm can be made explicit and the system becomes:

$$\begin{cases} A\Gamma + cV = c_0 V \\ c = \frac{\omega\Gamma}{b(1-\omega\Gamma)} \end{cases} \tag{A2}$$

From which, by substitution in the mass balance, the following second-degree equation in Γ can be obtained:

$$Ab\omega\,\Gamma^2 - (bA + \omega V + bc_0\omega V)\Gamma + bc_0 V = 0 \tag{A3}$$

and solved with the condition, $\omega\Gamma < 1$, which is satisfied by the solution with the minus sign.

For more complicated isotherms (Frumkin, 2-states), where an explicit relationship between c and Γ is not provided, numerical schemes must instead be adopted to solve the above set of Equation (A1).

Concerning the complete emulsification of an oil volume V_{oil} in a volume V of water, as a first approximation we can assume the total area of the droplets given by:

$$A = \frac{3}{R}V_{\text{oil}} \tag{A4}$$

where R is the average radius of the oil droplets. Introducing this area, together with the volume fraction $\Phi = V_{\text{oil}}/V$, the mass balance reads:

$$c + \frac{3}{R}\Phi\,\Gamma = c_0 \tag{A5}$$

In the case the adsorption process co-exists with surfactant partitioning between the volume of water V and the volume of oil V_{oil}, the mass balance is:

$$A\Gamma + cV + kcV_{\text{oil}} = c_0 V \tag{A6}$$

where $k = c_{\text{oil}}/c_{\text{water}}$ is the partition coefficient and c_0 and c refer to the concentrations in water.

After defining $\alpha = (1 + kV_{\text{oil}}/V)$, this equation can be recast as:

$$A\Gamma + \alpha cV = c_0 V \tag{A7}$$

Which allows the above equations for the depletion in the absence of partitioning to be easily adapted to account for partitioning.

The values of Γ, calculated using the described approach, allow estimating the realistic surfactant coverage, $\omega\Gamma$, for the droplets in the emulsion, which for the systems investigated here are reported in Table A1.

More accurate values for A can be obtained by considering the drop size distribution. If the number of drops N_i with the radius R_i, normalized on the total number of drops N_T, is distributed accordingly to $N_i/N_T = f_i(R_i)$, the total drop volume is given by:

$$V_{\text{oil}} = \sum_i N_i \frac{4}{3}\pi R_i{}^3 = N_T \sum_i f_i \frac{4}{3}\pi R_i{}^3 \tag{A8}$$

Thus

$$N_T = \frac{V_{\text{oil}}}{\sum_i f_i \frac{4}{3}\pi R_i{}^3} \tag{A9}$$

The total droplet area is thus given by:

$$A = \sum_i N_i 4\pi R_i{}^2 = N_T \sum_i f_i 4\pi R_i{}^2 = 3V_{\text{oil}} \frac{\sum_i f_i R_i{}^2}{\sum_i f_i R_i{}^3} \tag{A10}$$

So that, the equation equivalent to the mass balance A5 reads:

$$c + 3\Phi \frac{\sum_i f_i R_i{}^2}{\sum_i f_i R_i{}^3} \Gamma = c_0 \tag{A11}$$

For the emulsions studied here, the resulting size distributions are however always quite narrow, so that the use of Equation (A11), does not modify substantially the values of the coverage reported in Table A1.

Table A1. Depleted concentrations of the continuous phase (c) and the corresponding surface coverages of the droplets after emulsification. c_0 is the concentration of the aqueous solution before emulsification.

c_0 (M)	Average Drop Radius (µm)	c (M)	Surface Coverage
	Tween 80		
8.0×10^{-7}	8.6	3.6×10^{-10}	1.2×10^{-3}
1.0×10^{-6}	7.7	4.1×10^{-10}	1.4×10^{-3}
4.0×10^{-6}	6.6	1.4×10^{-9}	4.7×10^{-3}
8.0×10^{-6}	6.3	2.7×10^{-9}	9.0×10^{-3}
	Saponin		
6.1×10^{-6}	6.1	4.9×10^{-9}	0.015
3.0×10^{-5}	6.5	2.7×10^{-8}	0.078
6.1×10^{-5}	5.6	5.3×10^{-8}	0.138
1.8×10^{-4}	5.3	2.0×10^{-7}	0.381
3.0×10^{-4}	4.5	4.0×10^{-7}	0.550
	Citronellol Glucoside		
3.1×10^{-6}	8.7	1.1×10^{-6}	1.6×10^{-3}
3.1×10^{-4}	5.5	9.1×10^{-5}	0.115
6.3×10^{-4}	5.0	1.8×10^{-4}	0.207
1.6×10^{-3}	8.5	7.3×10^{-4}	0.511

References

1. Driscoll, D.F.; Nehne, J.; Peterss, H.; Franke, R.; Bistrian, B.R.; Niemann, W. The influence of medium-chain triglycerides on the stability of all-in-one formulations. *Int. J. Pharm.* **2002**, *240*, 1–10. [CrossRef]

2. Chatzidaki, M.D.; Mateos-Diaz, E.; Leal-Calderon, F.; Xenakis, A.; Carrière, F. Water-in-oil microemulsions versus emulsions as carriers of hydroxytyrosol: An in vitro gastrointestinal lipolysis study using the pHstat technique. *Food Funct.* **2016**, *7*, 2258–2269. [CrossRef] [PubMed]

3. Ragelle, H.; Crauste-Manciet, S.; Seguin, J. Nanoemulsion formulation of fisetin improves bioavailability and antitumour activity in mice. *Int. J. Pharm.* **2012**, *427*, 452–459. [CrossRef] [PubMed]

4. Terjung, N.; Löffler, M.; Gibis, M.; Hinrichs, J.; Weiss, J. Influence of droplet size on the efficacy of oil-in-water emulsions loaded with phenolic antimicrobials. *Food Funct.* **2012**, *3*, 290–301. [CrossRef]

5. Oleszek, W.; Hamed, A. Saponin-Based Surfactants. In *Surfactants from Renewable Resources*; Kjellin, M., Johansson, I., Eds.; John Wiley & Sons, Ltd.: Hoboken, NJ, USA, 2010; pp. 239–249. [CrossRef]

6. Güçlü-Üstündağ, Ö.; Mazza, G. Saponins: Properties, applications and processing. *Crit. Rev. Food Sci. Nutr.* **2007**, *47*, 231–258. [CrossRef]

7. Böttcher, S.; Drusch, S. Saponins—Self-assembly and behaviour at aqueous interfaces. *Adv. Colloid Interface Sci.* **2017**, *243*, 105–113. [CrossRef]

8. Jurado Gonzalez, P.; Sörensen, P.M. Characterization of saponin foam from Saponaria officinalis for food applications. *Food Hydrocoll.* **2020**, *101*, 105541. [CrossRef]

9. Giménez-Ribes, G.; Habibi, M.; Sagis, L.M.C. Interfacial rheology and relaxation behavior of adsorption layers of the triterpenoid saponin Escin. *J. Colloid Interface Sci.* **2020**, *563*, 281–290. [CrossRef]

10. Ulaganathan, V.; Del Castillo, L.; Webber, J.L.; Ho, T.T.M.; Ferri, J.K.; Krasowska, M.; Beattie, D.A. The influence of pH on the interfacial behaviour of Quillaja bark saponin at the air-solution interface. *Colloids Surf. B* **2019**, *176*, 412–419. [CrossRef]

11. Santini, E.; Jarek, E.; Ravera, F.; Liggieri, L.; Warszynski, P.; Krzan, M. Surface properties and foamability of saponin and saponin-chitosan systems. *Colloids Surf. B* **2019**, *181*, 198–206. [CrossRef]

12. Zhu, L.; Xu, Q.; Liu, X.; Xu, Y.; Yang, L.; Wang, S.; Li, J.; Ma, T.; Liu, H. Oil-water interfacial behavior of soy β-conglycinin–soya saponin mixtures and their effect on emulsion stability. *Food Hydrocoll.* **2020**, *101*, 105531. [CrossRef]

13. Wei, Y.; Tong, Z.; Dai, L.; Ma, P.; Zhang, M.; Liu, J.; Mao, L.; Yuan, F.; Gao, Y. Novel colloidal particles and natural small molecular surfactants co-stabilized Pickering emulsions with hierarchical interfacial structure: Enhanced stability and controllable lipolysis. *J. Colloid Interface Sci.* **2020**, *563*, 291–307. [CrossRef] [PubMed]

14. Huang, T.; Tu, Z.; Zou, Z.; Shangguan, X.; Wang, H.; Bansal, N. Glycosylated fish gelatin emulsion: Rheological, tribological properties and its application as model coffee creamers. *Food Hydrocoll.* **2020**, *102*, 105552. [CrossRef]

15. Riquelme, N.; Zúñiga, R.N.; Arancibia, C. Physical stability of nanoemulsions with emulsifier mixtures: Replacement of Tween 80 with quillaja saponin. *LWT Food Sci. Technol.* **2019**, *111*, 760–766. [CrossRef]

16. Bak, A.; Podgórska, W. Interfacial and surface tensions of toluene/water and air/water systems with nonionic surfactants Tween 20 and Tween 80. *Colloids Surf. A* **2016**, *504*, 414–425. [CrossRef]

17. Zhu, Z.; Wen, Y.; Yi, J.; Cao, Y.; Liu, F.; McClements, D.J. Comparison of natural and synthetic surfactants at forming and stabilizing nanoemulsions: Tea saponin, Quillaja saponin, and Tween 80. *J. Colloid Interface Sci.* **2019**, *536*, 80–87. [CrossRef]

18. Kumar, N.; Mandal, A. Thermodynamic and physicochemical properties evaluation for formation and characterization of oil-in-water nanoemulsion. *J. Mol. Liq.* **2018**, *266*, 147–159. [CrossRef]

19. Leal-Calderon, F.; Schmitt, V.; Bibette, J. *Emulsion Science, Basic Principles*; Springer: Berlin/Heidelberg, Germany, 2007; pp. 143–172. ISBN 978-0-387-39682-8.

20. Georgieva, D.; Schmitt, V.; Leal-Calderon, F.; Langevin, D. On the possible role of surface elasticity in emulsion stability. *Langmuir* **2009**, *25*, 5565–5573. [CrossRef]

21. Schmitt, V.; Cattelet, C.; Leal-Calderon, F. Coarsening of Alkane-in-water emulsions stabilized by nonionic poly(oxyethylene) surfactants: The role of molecular permeation and coalescence. *Langmuir* **2004**, *20*, 46–52. [CrossRef]

22. Taisne, L.; Walstra, P.; Cabane, B. Transfer of oil between emulsion droplets. *J. Colloid Interface Sci.* **1996**, *184*, 378–390. [CrossRef]

23. Kabalnov, A.S.; Makarov, K.N.; Pertzov, A.V.; Shchukin, E.D. Ostwald ripening in emulsions: 2. Ostwald ripening in hydrocarbon emulsions: Experimental verification of equation for absolute rates. *J. Colloid Interface Sci.* **1990**, *138*, 98–104. [CrossRef]

24. Boos, J.; Preisig, N.; Stubenrauch, C. Dilational surface rheology studies of n-dodecyl-β-D-maltoside, hexaoxyethylene dodecyl ether, and their 1:1 mixture. *Adv. Colloid Interface Sci.* **2013**, *197–198*, 108–117. [CrossRef] [PubMed]

25. Llamas, S.; Santini, E.; Liggieri, L.; Salerni, F.; Orsi, D.; Cristofolini, L.; Ravera, F. Adsorption of sodium dodecyl sulfate at water-dodecane interface in relation to the oil in water emulsion properties. *Langmuir* **2018**, *34*, 5978–5989. [CrossRef] [PubMed]

26. Chung, C.; Sher, A.; Rousset, P.; Decker, E.A.; McClements, D.J. Formulation of food emulsions using natural emulsifiers: Utilization of quillaja saponin and soy lecithin to fabricate liquid coffee whiteners. *J. Food Eng.* **2017**, *209*, 1–11. [CrossRef]

27. Taarji, N.; da Rabelo Silva, C.A.; Khalid, N.; Gadhi, C.; Hafidi, A.; Kobayashi, I.; Neves, M.A.; Isoda, H.; Nakajima, M. Formulation and stabilization of oil-in-water nanoemulsions using a saponins-rich extract from argan oil press-cake. *Food Chem.* **2018**, *246*, 457–463. [CrossRef]

28. Bai, L.; McClements, D.J. Formation and stabilization of nanoemulsions using biosurfactants: Rhamnolipids. *J. Colloid Interface Sci.* **2016**, *479*, 71–79. [CrossRef]

29. Wojciechowski, K. Surface activity of saponin from Quillaja bark at the air/water and oil/water interfaces. *Colloids Surf. B* **2013**, *108*, 95–102. [CrossRef]

30. Stanimirova, R.; Marinova, K.; Tcholakova, S.; Denkov, N.D.; Stoyanov, S.; Pelan, E. Surface rheology of saponin adsorption layers. *Langmuir.* **2011**, *27*, 12486–12498. [CrossRef]

31. Mitra, S.; Dungan, S.R. Micellar properties of quillaja saponin. 1. Effects of temperature, salt, and pH on solution properties. *J. Agric. Food Chem.* **1997**, *45*, 1587–1595. [CrossRef]

32. Kairaliyeva, T.; Aksenenko, E.V.; Mucic, N.; Makievski, A.V.; Fainerman, V.B.; Miller, R. Surface tension and adsorption studies by drop profile analysis tensiometry. *J. Surfactants Deterg.* **2017**, *20*, 1225–1241. [CrossRef]

33. Ravera, F.; Loglio, G.; Kovalchuk, V.I. Interfacial dilational rheology by oscillating bubble/drop methods. *Curr. Opin. Colloid Interface Sci.* **2010**, *15*, 217–228. [CrossRef]

34. Loglio, G.; Pandolfini, P.; Liggieri, L.; Makievski, A.V.; Ravera, F. *Bubble and Drops Interfaces*; Miller, R., Liggieri, L., Eds.; Brill: Leiden, The Netherlands, 2011; pp. 7–38.

35. Gaillard, T.; Rochéa, M.; Honorez, C.; Jumeau, M.; Balan, A.; Jedrzejczyk, C.; Drenckhan, W. Controlled foam generation using cyclic diphasic flows through a constriction. *Int. J. Multiph. Flow* **2017**, *96*, 173–187. [CrossRef]

36. Fainerman, V.B.; Miller, R.; Wustneck, R.; Makievski, A.V. Adsorption isotherm and surface tension equation for a surfactant with changing partial molar area. 1. Ideal surface layer. *J. Phys. Chem.* **1996**, *100*, 7669–7675. [CrossRef]

37. Fainerman, V.B.; Zholob, S.A.; Lucassen-Reynders, E.H.; Miller, R. Comparison of various models describing the adsorption of surfactant molecules capable of interfacial reorientation. *J. Colloid Interface Sci.* **2003**, *261*, 180–183. [CrossRef]

38. Ravera, F.; Ferrari, M.; Liggieri, L. Adsorption and partitioning of surfactants in liquid–liquid systems. *Adv. Colloid Interface Sci.* **2000**, *88*, 129–177. [CrossRef]

39. Ravera, F.; Liggieri, L.; Ferrari, M.; Miller, R.; Passerone, A. Measurement of the partition coefficient of surfactants in water/oil systems. *Langmuir* **1997**, *13*, 4817–4820. [CrossRef]

40. Fainerman, V.B.; Sharipova, A.A.; Aidarova, S.B.; Kovalchuk, V.I.; Aksenenko, E.V.; Makievski, A.V.; Miller, R. Direct determination of the distribution coefficient of tridecyl dimethyl phosphine oxide between water and hexane. *Colloids Interfaces* **2018**, *2*, 28. [CrossRef]

41. Ravera, F.; Ferrari, M.; Liggieri, L. Modelling of dilational visco-elasticity of adsorbed layers with multiple kinetic processes. *Colloids Surf. A* **2006**, *282*, 210–216. [CrossRef]

42. Ravera, F.; Ferrari, M.; Liggieri, L.; Loglio, G.; Santini, E.; Zanobini, A. Liquid-liquid interfacial properties of mixed nanoparticle-surfactant systems. *Colloids Surf. A* **2008**, *323*, 99–108. [CrossRef]

43. Santini, E.; Liggieri, L.; Sacca, L.; Clausse, D.; Ravera, F. Interfacial rheology of Span 80 adsorbed layers at paraffin oil–water interface and correlation with the corresponding emulsion properties. *Colloids Surf. A* **2007**, *309*, 270–279. [CrossRef]
44. Whitby, C.P.; Fornasiero, D.; Ralston, J.; Liggieri, L.; Ravera, F. Properties of fatty amine-silica nanoparticle interfacial layers at the hexane-water interface. *J. Phys. Chem. C* **2012**, *116*, 3050–3058. [CrossRef]